Spontaneous Motion of Nanorobots Inspired Computational Technology for Tumor Boundary Exploration

Shaolong Shi[1(✉)] and Yifan Chen[2]

[1] Yangtze Delta Region Institute (Quzhou), University of Electronic Science and Technology of China, Quzhou, China
shishaolong@csj.uestc.edu.cn

[2] School of Life Science and Technology, University of Electronic Science and Technology of China, Chengdu, China

Abstract. We recently introduced a new and innovative framework named "*in vivo* computation" by modeling the tumor targeting problem as a natural computation problem. Nanorobots play the role of computing agents are guided by the information of biological gradient field (BGF) induced by the emerging of tumor for the searching of tumor location which is the optimal solution for the *in vivo* computational problem. To overcome the *in vivo* constraints encountered in previous research, which primarily concentrated on tumor detection, several computational strategies have been suggested for achieving tumor targeting. This work concentrates on the exploration of tumor boundary with nanorobots, which is a novel and valuable research point. To overcome this challenge, we resort to the spontaneous motion of nanorobots in liquid environment, where the local hydrodynamic flows are used to actuate the nanorobots to keep a balance to the effect of BGF. In order to showcase the efficacy of the proposed methods, we conduct *in silico* experiments across three BGF landscapes that vary in terms of their optimization complexity.

Keywords: Nanorobots · spontaneous motion · computational intelligence · tumor detection

1 Introduction

Due to the limited resolution of medical imaging devices over the past few decades, early tumor detection has posed a significant challenge in the biomedical field [1]. As information and communications technology (ICT) advances, an increasing number of innovative tools inspired by nature are coming into view [2]. In particular, the emergence of nanotechnology and nanomedicine has accelerated the development of precision medicine, offering promising prospects for addressing diverse medical conditions such as early tumor sensitization and targeting (TST), since Nobel laureate Richard P. Feynman delivered his influential speech titled "There's Plenty of Room at the Bottom" in 1959 [3, 4].

Y. Chen et al. (Eds.): BICT 2024, LNICST 592, pp. 154–160, 2025.
https://doi.org/10.1007/978-3-031-81599-7_15

1.1 Computational Nanobiosensing

The emergence of nanomedicine offers a clever approach to tackle some of the most intricate medical challenges, such as early tumor detection, which have been limited by conventional diagnostic and therapeutic methods. Nanorobots equipped with sensing, actuating, and signaling capabilities hold great promise for improving the efficacy of tumor detection [5]. For instance, drawing inspiration from the swimming behavior of bacterial flagella, Ghosh and Fischer have invented a helical glass propeller coated with cobalt that can attain a speed of approximately 40 μm/s. Despite the research into nanorobots with various propulsion methods, magnetic nanorobots stand out as the most promising due to their fuel-free operation and ability to penetrate deep tissues under an external magnetic field, making them suitable for *in vivo* imaging and actuation [6]. However, despite its potential, this method falls short in achieving early targeting of microscopic tumors because it necessitates prior knowledge of the tumor's location, which is unavailable until the detection process has been completed (the "chicken-or-egg causality dilemma") [7].

To tackle the challenges that lie beyond the capabilities of traditional biomedical technologies, a novel paradigm known as computational nanobiosensing (CONA) has been proposed [8]. Within the scope of CONA, we introduced an innovative framework of *in vivo* computation, where the process of tumor targeting is transformed into a computational methodology to address the challenge of detecting microscopic tumors [9]. Nanorobots are regarded as computational agents tasked with finding the global optimal solution, which in this case is the tumor location. The tumor-induced biological gradient field (BGF) serves as the optimization landscape, providing auxiliary information to facilitate the targeting process. Nanorobots, equipped with targeted strategies, navigate through high-risk tissue to locate the tumor site.

1.2 Literature Review

Since the presentation of "*in vivo* computation", several contributions have been done about the tumor targeting strategies design by taking consideration into the practical constraints of internal environment. Taking into account the practical constraint posed by an external uniform magnetic field for controlling nanorobot movement, we introduced the Orthokinetic Gravitational Search Algorithm (OGSA), which is grounded in several innovative evolutionary strategies in [9]. It was demonstrated that OGSA based on weak priority evolution strategy (WP-ES) had the best performance on TST. In [10], we introduced a unique computational principle, termed the tension-relaxation (T-R) principle, for equilibrating the movements of nanorobots across each

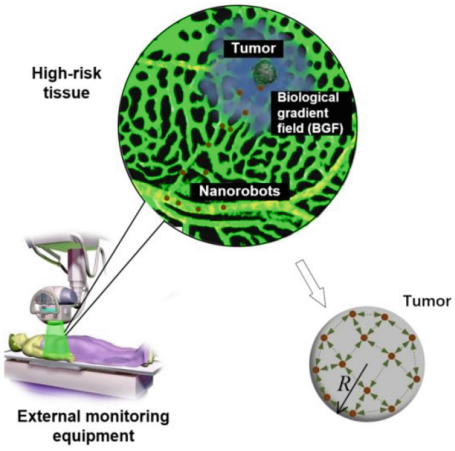

Fig. 1. Graphical representation of the nanorobots exploring the tumor boundary.

control and tracking cycle. It emphasized the balance between nanorobot control and tracking operations, integral components of *in vivo* computation, where the control operation was dedicated to efficiently locating the tumor, while the tracking mode facilitated the collection of information regarding BGF. In [11], we proposed an exponential evolution mechanism to modify the step size of the nanorobots during each period of actuation. From a computational standpoint, the exponential evolution mechanism enhances exploration capabilities at the start of the search and optimizes exploitation at the end, enabling swift and precise tumor detection.

Previous research primarily concentrated on the tumor targeting process involving nanorobots once injected into the body, with limited attention given to the targeting outcomes. This work will concentrate on the exploration of tumor boundary with nanorobots (as shown in Fig. 1), which is a novel and valuable research point. Thus, we resort to the property of autonomous nanorobots, which can generate spontaneous motion in liquid environment. We use the local hydrodynamic flows to actuate the nanorobots to keep a balance to the effect of BGF. The state of the balance is just the exploration result of nanorobots.

2 Autonomous *In Vivo* Computation

Self-propelled nanorobotics powered by chemical fuel (e.g., SiO_2/Ir Janus micromotors) exhibit stable autonomous movement in a consistent oblique head-down position near a substrate, generating powerful and steady convergent phoretic flows that emit robust, long-distance hydrodynamic signals. Hence, nanorobots within a wide vicinity can detect each other through hydrodynamic signals and subsequently trigger an "approach-hit-and-run" mechanism. This involves a swift transition from random to directed movement towards each other at a distance, followed by a dramatic speed-up and reorientation to escape after colliding [12]. Inspired by this phenomenon, we propose an *in vivo* computational technology for tumor boundary exploration in this paper.

2.1 Problem Formulation

In the context of *in vivo* computation, nanorobots acting as computational agents navigate through high-risk tissue to locate the tumor lesion, which represents the optimal solution to the optimization problem at hand. The mathematical model is expressed as below:

$$f(\boldsymbol{x}, A) = f_{\mathrm{T}}(\boldsymbol{x}) + \epsilon(\boldsymbol{x}, A), \tag{1}$$

and

$$\boldsymbol{x}^{*} = \underset{\boldsymbol{x}}{\operatorname{argmax}} f(\boldsymbol{x}, A), \tag{2}$$

where f denotes the objective function measured by agent A; f_{T} signifies the *true* objective function that represents the BGF; ϵ is the measuring error of agent A; $\boldsymbol{x}^{*}$ is the global optimum of the problem. Thus, the exploration of tumor boundary can be interpreted as searching the region of all the $\boldsymbol{x}^{*}$ as many as possible.

2.2 Biological Gradient Field Representation

Given that current research has yet to establish a widely accepted and accurate quantitative model of BGF that can represent the diverse biological information surrounding tumors, we utilize several representative optimizable functions presented in Eqs. (3)–(5) in this study to capture the essential characteristics of BGF landscapes. All the BGF landscapes align generally with the qualitative observations reported in previous work and offer valuable insights into assessing the proposed method for exploring tumor boundaries [13]. Although additional landscapes could be utilized, it is practical to employ these as representations to test the proposed approach in this paper (Fig. 2).

- Landscape I

$$f_{\mathrm{T}}(\boldsymbol{x}) = \begin{cases} 1, & \sqrt{x^2+y^2} < 5 \\ 1-\left(x^2+y^2+10\right)/85, & \sqrt{x^2+y^2} \geq 5. \end{cases} \tag{3}$$

- Landscape II

$$f_{\mathrm{T}}(\boldsymbol{x}) = \begin{cases} 1, \sqrt{x^2+y^2} < 5 \\ 4/3\exp\left(-\sqrt{2x^2+2y^2}/10\right) - e/15 - 1/3 \\ +1/15\exp(1/2(\cos(2\pi x)+\cos(2\pi y))), \sqrt{x^2+y^2} \geq 5. \end{cases} \tag{4}$$

- Landscape III

$$f_{\mathrm{T}}(\boldsymbol{x}) = \begin{cases} 1, & \sqrt{x^2+y^2} < 5 \\ 1/100\left[10(\cos(2\pi x)+\cos(2\pi y)) - x^2 - y^2\right] + 0.65, & \sqrt{x^2+y^2} \geq 5. \end{cases} \tag{5}$$

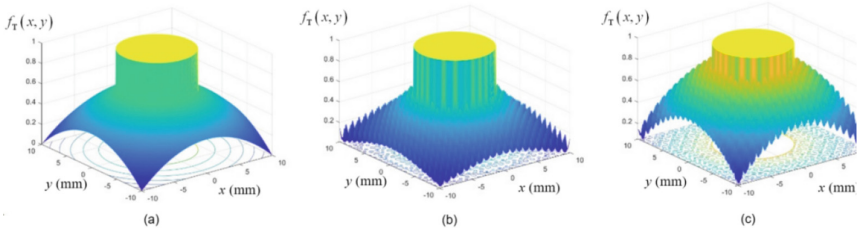

Fig. 2. Three illustrative BGF landscapes, each exhibiting varying levels of complexity. (a) Landscape I with smooth change; (b) Landscape II with fluctuating change; (c) Landscape III with many local minima.

2.3 Nanorobot Motion Mechanisms

- Cooperation mechanism

Resulting from the response of nanorobots with the BGF landscape, the nanorobots will coordinate migration, which is the fundamental motion mechanism of autonomous nanorobots. Assuming N nanorobots are deployed in the search space for tumor targeting with their locations represented by $\boldsymbol{x}_1, \boldsymbol{x}_2, \cdots, \boldsymbol{x}_N$, the values of sensed BGF with them are $f(\boldsymbol{x}_1), f(\boldsymbol{x}_2), \cdots, f(\boldsymbol{x}_N)$. Furthermore, K neighbors of a nanorobot are selected according to the nearest neighbor criterion. The specific nanorobot moves in cooperation with its neighbors in the way that a neighbor with high BGF value will adsorb it, while one with low BGF value will repel it. Thus, the migration direction of the specific nanorobot can be calculated according to:

$$\boldsymbol{u} = \frac{\boldsymbol{x}_n - \boldsymbol{x}_k}{\|\boldsymbol{x}_n - \boldsymbol{x}_k\|}, \tag{6}$$

where $\boldsymbol{x}_n$ is the location of a specific nanorobot in the swarm with $i = 1,2, \cdots, N$, and $\boldsymbol{x}_k$ is the location of its neighbor with $i = 1,2, \cdots, K$.

The effects of the neighbors on the specific nanorobot is:

$$\mathcal{H} = \sum\nolimits_{i=1}^{K} \frac{\Delta f_{n,k}}{[\|\boldsymbol{x}_n - \boldsymbol{x}_k\|/d_0]^l} \boldsymbol{u}, \tag{7}$$

where $\Delta f_{n,k} = f(\boldsymbol{x}_k) - f(\boldsymbol{x}_n)$ is the difference of BGF values perceived by the specific nanorobot and its neighbor; d_0 is a normalization factor; l is the path loss index.

The location update of the nanorobot with cooperation mechanism is:

$$\boldsymbol{x}_{n,t+1} = \boldsymbol{x}_{n,t} + \gamma \cdot \mathcal{H}, \tag{8}$$

where γ is the unit step size. Then, all the nanorobots of the swarm update their locations according to this collaboration mechanism.

- Competition mechanism

Nanorobots will generate strong, steady converging phoretic flows while autonomously moving, thereby emitting robust hydrodynamic signals, which will initiate an "approach-hit-and-run" response for neighboring nanorobots within the perception distance. This phenomenon can be seen as an competition mechanism for nanorobots as they will exhibit significant repulsion towards each other within a specific range. The effect of repulsion can be calculated as follows:

$$T(t) = \sum\nolimits_{i=1}^{K} \left[\frac{q(t)}{8\pi\lambda\|\boldsymbol{x}_n - \boldsymbol{x}_k\|^3} \cdot \Gamma(\|\boldsymbol{x}_n - \boldsymbol{x}_k\| - R) + \frac{q(t)}{8\pi\lambda R^3} \cdot \Gamma(R - \|\boldsymbol{x}_n - \boldsymbol{x}_k\|) \right] \boldsymbol{u} \tag{9}$$

where $\Gamma(x) = \begin{cases} x, & x \geq 0 \\ 0, & x < 0 \end{cases}$; $q(t)$ is the polarization intensity of the nanorobot; λ is the viscosity coefficient of the blood; R is the radius of repulsion.

The location update of the nanorobot with competition mechanism is:

$\boldsymbol{x}_{n,t+1} = \boldsymbol{x}_{n,t} + \gamma \cdot T(t)$, , (10).

Thus, the nanorobots move in the search space to target the tumor and explore the tumor region by using the cooperation and competition mechanisms autonomously.

3 Experimental Analysis

To characterize the result of tumor boundary exploration by using autonomous computational nanobiosensing technology, we carry out several numerical simulation experiments in Landscape I, II, and III.

In the experiments, 50 agents are utilized as autonomous nanorobots in the search space, where a circle region with the radius of 5 mm in the center represents the tumor region. The number of neighbors K is 10, the movement step size γ is 0.05 mm. Figure 3 shows the procedure of tumor boundary in Landscape I (Landscape II and III have the similar results which will not be over-expressed here). As shown in Fig. 3a, the initial distribution of nanorobots is in the bottom left corner of the search space. All the nanorobots will move with the effect of cooperation mechanism and competition mechanism. With the process going on, the nanorobots will detect the tumor region more and more as shown in Fig. 3b. Figure 3c shows the final result of the tumor boundary exploration with a state of balance reached by cooperation mechanism and competition mechanism. It can be seen that all the nanorobots are located dispersively in the tumor region and some are distributed on the tumor boundary, which indicates a desired exploration result of the tumor boundary.

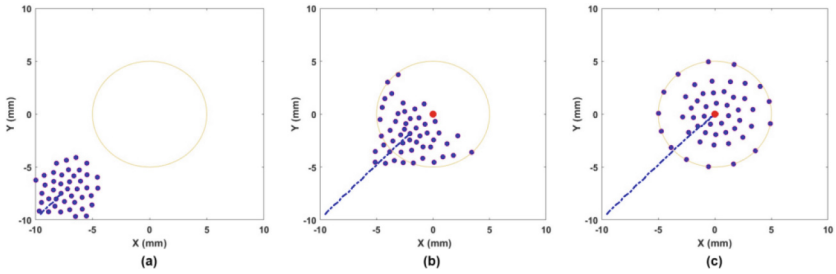

Fig. 3. Distributions of nanorobots in Landscape I at three different moments: (a) the initial moment, (b) the intermediate moment, (c) the terminal moment.

Furthermore, we propose metrics (M and D) to quantize the result of tumor boundary exploration. M is the ratio of nanorobot number that locate on the tumor boundary. D is the variance of all the nanorobot locations. The final computational results are shown in Table 1.

Table 1. The quantization results of tumor boundary exploration.

Landscapes / Metrics	I	II	III
M	26%	28%	28%
D	5.621	5.884	5.676

4 Conclusion

We have proposed a novel approach of utilizing the cooperation and competition mechanisms of autonomous nanorobots to overcome the challenge of tumor boundary exploration, which is a significant research gap that has not been focused in the field of computational nanobiosensing. The *in silico* simulation outcomes confirm the efficacy of the proposed methodology with almost all the tumor boundary being located by the nanorobots that have a balance state of the cooperation and competition mechanisms.

Acknowledgment. This work is supported by the National Natural Science Foundation of China (Grant No. 62102071, 62472322), and the Municipal Government of Quzhou (Grant No. 2023D031).

References

1. Weinberg, R.A., Weinberg, R.A.: The biology of cancer. WW Norton & Company (2006)
2. Nakano, T.: Molecular communication. Cambridge University Press (2013)
3. Bhushan, B.: Introduction to nanotechnology. Springer Handbook of Nanotechnology, pp. 1–19 (2017)
4. Suhag, D., Thakur, P., Thakur, A.: Introduction to nanotechnology. Integrat. Nanomater. Appl. 1–17 (2023)
5. Li, J., Esteban-Fernández de Ávila, B., Gao, W., et al.: Micro/nanorobots for biomedicine: delivery, surgery, sensing, and detoxification. Sci. Robot. **2**(4), eaam6431 (2017)
6. Fischer, P., Ghosh, A.: Magnetically actuated propulsion at low Reynolds numbers: towards nanoscale control. Nanoscale **3**(2), 557–563 (2011)
7. Xu, J., Kang, D., Xu, M., et al. Multiphoton microscopic imaging of esophagus during the early phase of tumor progression. Scan. J. Scan. Microscop. **35**(6), 387–391 (2013)
8. Shi, S., Sharifi, N., Cheang, U.K., et al.: Perspective: computational nanobiosensing. IEEE Trans. Nanobiosci. **19**(2), 267–269 (2019)
9. Shi, S., Chen, Y., Yao, X.: In vivo computing strategies for tumor sensitization and targeting. IEEE Trans. Cybern. **52**(6), 4970–4980 (2020)
10. Shi, S., Sharifi, N., Chen, Y., et al.: Tension-relaxation in vivo computing principle for tumor sensitization and targeting. IEEE Trans. Cybern. **52**(9), 9145–9156 (2021)
11. Shi, S., Chen, Y., Yao, X., et al.: Exponential evolution mechanism for in vivo computation. Swarm Evol. Comput. **65**, 100931 (2021)
12. Cheng, Y., Mou, F., Yang, M., et al.: Long-range hydrodynamic communication among synthetic self-propelled micromotors. Cell Reports Phys. Sci. **3**(2), 100739 (2022)
13. Peng, S.J., Xiao, F.F., Chen, M.W., et al.: Tumor-microenvironment responsive nanomedicine for enhanced cancer immunotherapy. Adv. Sci. **9**(1), 2103836 (2022)